Title	Updated trade-off relationship between specific on-resistance and breakdown voltage in 4H-SiC{0001} unipolar devices
Author(s)	Kimoto, Tsunenobu
Citation	Japanese Journal of Applied Physics (2019), 58
Issue Date	2019-01
URL	http://hdl.handle.net/2433/236055
Right	© 2018 The Japan Society of Applied Physics. Content from this work may be used under the terms of the Creative Commons Attribution 4.0 license. Any further distribution of this work must maintain attribution to the author(s) and the title of the work, journal citation and DOI.
Type	Journal Article
Textversion	author

Japanese Journal of Applied Physics

The Japan Society of Applied Physics

BRIEF NOTE • **OPEN ACCESS**

Updated trade-off relationship between specific on-resistance and breakdown voltage in 4H-SiC{0001} unipolar devices

OPEN ACCESS

Japanese Journal of Applied Physics **58**, 018002 (2019)

https://doi.org/10.7567/1347-4065/aae896

BRIEF NOTE

Updated trade-off relationship between specific on-resistance and breakdown voltage in 4H-SiC{0001} unipolar devices

Tsunenobu Kimoto

Department of Electronic Science and Engineering, Kyoto University A1 Katsura, Nishikyo, Kyoto 615-8510, Japan

*E-mail: kimoto@kuee.kyoto-u.ac.jp

Received September 16, 2018; accepted October 11, 2018; published online November 6, 2018

The minimum specific on-resistance of 4H-SiC{0001} unipolar devices as a function of the breakdown voltage was updated based on latest studies on intrinsic physical properties, such as impact ionization coefficients. Both punch-through (PT) and nonpunch-through (NPT) structures were considered, because a PT structure generally gives a lower on-resistance at a given breakdown voltage. The minimum specific on-resistance of 1 kV 4H-SiC devices can be as low as 0.20 mΩ cm^2 at room temperature. An analytical expression for the relationship between the specific on-resistance and breakdown voltage is given. © 2018 The Japan Society of Applied Physics

Among various wide bandgap semiconductors, silicon carbide (SiC) exhibits several technological advantages, such as the availability of large-diameter (150 mm) wafers and wide range doping control of n- and p-type conductivity via either in situ doping or ion implantation.[1–6] A long carrier lifetime due to its indirect band structure is another inherent advantage of SiC for the development of ultrahigh-voltage bipolar devices.[7–10] Recent progress in SiC technology has triggered the production of 600–1700 V Schottky barrier diodes (SBDs) and metal-oxide-semiconductor field effect transistors (MOSFETs). 3300 V SiC devices have also been produced and implemented into high-power modules for traction applications.[11]

In development of SiC (and other wide bandgap semiconductors) power devices, the specific on-resistance (R_{on_sp}) experimentally obtained has often been compared with the "unipolar limit" of the material, which is a strong function of the breakdown voltage, to discuss the technological maturity.[12–16] The unipolar limit of one material has also been used to compare the potential of different materials.[17–19] In general, the unipolar limit is defined by the trade-off relationship between the specific resistance of a drift layer and the breakdown voltage (V_B).[20] However, unipolar limits of wide bandgap semiconductors previously reported have been rather inaccurate and the unipolar limit is different in different papers. This problem is mainly caused by the following reasons: (i) the intrinsic physical properties of a material such as mobility (μ) and critical electric field strength (E_{crit}) have not been well clarified. In addition, these properties were often assumed to be independent of the doping density, although, both are strongly doping-dependent. (ii) The unipolar limit has usually been calculated for a NPT structure by the following equation.[20]

$$R_{on\_sp} = 4V_B^2/(\varepsilon_s \mu E_{crit}^3). \quad (1)$$

Here, ε_s is the permittivity of the semiconductor. However, it is well known that a PT structure usually gives a significantly lower drift resistance than an NPT structure at a given breakdown voltage;[21] further, NPT structures have almost never been employed for production of power devices. Therefore, the unipolar limit of wide bandgap semiconductors must be revisited while taking account of these factors. Although a similar analysis has been published,[2] the physical properties adopted in the previous analysis is not the latest and more updated results are presented in this paper. Furthermore, basic device physics behind the obtained results is discussed.

In this study, the author examined the unipolar limit of 4H-SiC{0001} power devices, considering the latest physical properties and PT structures. Here, the 4H polytype of SiC is the most promising among many polytypes owing to its high electron mobility, high critical electric field strength, and the availability of single crystalline wafers of reasonably high quality.[1,2] 4H-SiC devices on nonbasal planes such as (11$\bar{2}$0) are less attractive because of the lower critical field strength along ⟨11$\bar{2}$0⟩[22,23] and the difficulty in the growth of large ingots. Thus, this study focuses on 4H-SiC unipolar devices fabricated on {0001}. An n-type drift region is exclusively considered since p-type SiC-based unipolar devices exhibit much higher on-resistance due to the low hole mobility and incomplete ionization of acceptors at room temperature. It should be noted that a "super-junction" structure,[24] the specific on-resistance of which can be remarkably reduced by specially-designed structures, is not considered in this study.

Figure 1 depicts the critical electric field strength of 4H-SiC ⟨0001⟩ as a function of the doping density, which was calculated by using the latest impact ionization coefficients. The impact ionization coefficients are given by the following equations.[25]

$$\text{Electron: } \alpha(E) = 1.43 \times 10^5 \exp\left\{-\left(\frac{4.93 \times 10^6}{E}\right)^{2.37}\right\} \text{cm}^{-1} \quad (2)$$

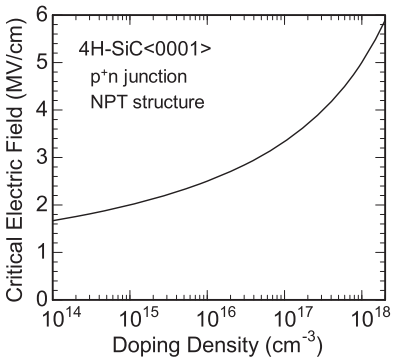

Fig. 1. Critical electric field strength of 4H-SiC⟨0001⟩ as a function of the doping density, which was calculated using the latest impact ionization coefficients.[25] Nonpunch-through (NPT) p^+n junctions are considered.

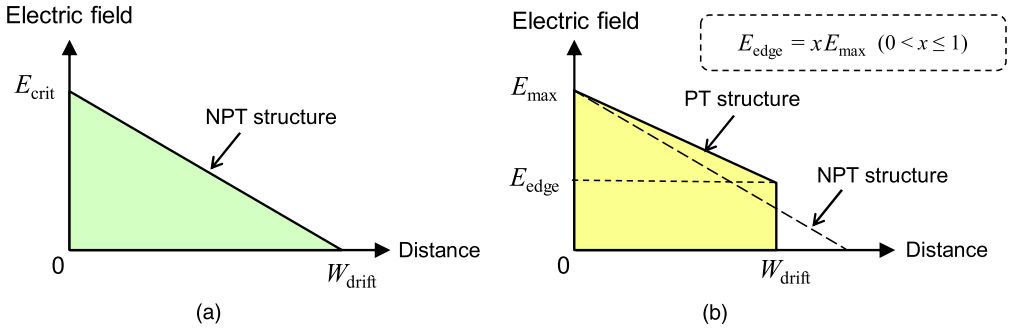

Fig. 2. (Color online) Profiles of the electric field strength inside a drift layer at breakdown for (a) nonpunch-through (NPT) and (b) punch-through (PT) structures.

$$\text{Hole: } \beta(E) = 3.12 \times 10^6 \exp\left\{-\left(\frac{1.18 \times 10^7}{E}\right)^{1.02}\right\} \text{cm}^{-1} \quad (3)$$

where E is the electric field strength in the unit of V cm^{-1}. The critical field strength significantly increases by increasing the doping density, as in the case of other semiconductors: The critical field strengths are 2.00, 2.50, and 3.34, and 5.01 MV cm^{-1} at doping densities of 1×10^{15}, 1×10^{16}, 1×10^{17}, and 1×10^{18} cm^{-3}, respectively, at room temperature.[26] One should also consider that this critical electric field strength is valid only in the case of NPT structures. When the targeted device possesses a PT structure, the breakdown voltage must be determined by either calculation of ionization integral[20] or device simulation. The author confirmed that the ionization integral and device simulation (Synopsis, DESSIS) give an almost identical breakdown voltage for a given structure of SiC.

Figure 2 schematically plots the profiles of the electric field strength inside a drift layer at breakdown for (a) NPT and (b) PT structures. Here, it was assumed that the drift layer is uniformly doped along the depth. In the case of the NPT structure, the maximum electric field strength at breakdown (E_{max}) is equivalent to E_{crit} at the doping density and the thickness of the drift layer is designed to be the maximum width of the space-charge region. Thus, the breakdown voltage of this junction and the minimum drift resistance are uniquely determined once the doping density is given. The situation is more complicated in the case of PT structures shown in Fig. 2(b). There exist many combinations of the doping density and thickness of the drift layer which yield the same breakdown voltage. Furthermore, E_{max} is slightly higher than E_{crit} at the same doping density because the thickness of the space-charge region is smaller than that of the NPT structure. It has been suggested that the drift resistance becomes a minimum when the electric field strength at the edge of the drift region, which is denoted by E_{edge} in Fig. 2(b), is equal to $(1/3)E_{max}$ under an assumption that the critical electric field strength and mobility are independent of the doping density.[21] Therefore, the author calculated the drift resistance and breakdown voltage for various PT structures, where the thickness of a drift layer was gradually varied while keeping the doping density constant so that E_{edge} was changed in the range from about $0.2E_{max}$ to $0.4E_{max}$. Then this calculation was repeated by changing the doping density step-by-step. Based on this extensive calculation, a best trade-off relationship between the drift resistance and the breakdown voltage (a lowest drift resistance at a specified breakdown voltage) was determined. In this calculation, the breakdown voltage for each PT structure was determined by calculating the ionization integral using the impact ionization coefficients given by Eqs. (2) and (3).

Regarding the electron mobility of 4H-SiC, it is known that the mobility along ⟨0001⟩ ($\mu_{//}$) is about 14%–17% higher than that perpendicular to ⟨0001⟩ ($\mu_{\perp}$).[27] In the author's group, Hall effect measurements were performed on n-type/p-type multi-epitaxial layers grown on a 4H-SiC(11$\bar{2}$0) substrate. The intermediate p-type layer was grown for electrical isolation of the top n-type layer from the n-type substrate. Long Hall-bar configurations were formed along ⟨0001⟩ and [1$\bar{1}$00] on the same epitaxial samples, and the Hall mobility was extracted by assuming a Hall scattering factor of unity. For example, the electron mobility along ⟨0001⟩ was determined to be 912 cm^2 V^{-1} s^{-1}, whereas that along [1$\bar{1}$00] was 784 cm^2 V^{-1} s^{-1} at a donor density of 2.4×10^{16} cm^{-3}, indicating 16% higher mobility along ⟨0001⟩. Almost the same anisotropy (16% difference) in electron mobility was observed for epitaxial layers with donor densities of 8.1×10^{16} and 1.6×10^{17} cm^{-3}. These results and the mobility data obtained from conventional 4H-SiC{0001} samples are plotted by open squares and closed circles, respectively, in Fig. 3. Since the donor density dependence of electron mobility perpendicular to ⟨0001⟩ in 4H-SiC has been established,[2,28] the electron mobility along ⟨0001⟩, which determines the drift resistance of 4H-SiC {0001} devices, was calculated by using the following equation, assuming that the 16% difference is maintained irrespective of the donor density.

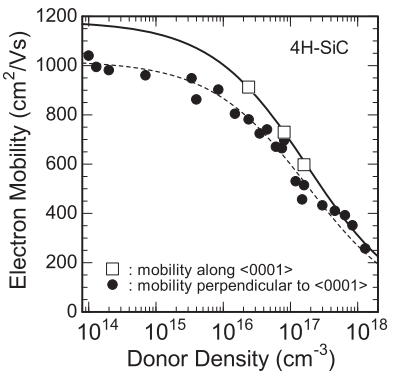

Fig. 3. Donor density dependence of electron mobility in 4H-SiC. The mobilities along ⟨0001⟩ ($\mu_{//}$) and perpendicular to ⟨0001⟩ ($\mu_{\perp}$) experimentally obtained are plotted by open squares and closed circles, respectively. The dashed line denotes the fitting curve for $\mu_{\perp}$ experimentally obtained.[2] The solid line represents the donor density dependence of $\mu_{//}$, assuming that $\mu_{//}$ is 16% higher than $\mu_{\perp}$ irrespective of the donor density.

$$\mu_{//} = \frac{1180}{1 + (N_D/1.8 \times 10^{17})^{0.6}}\ \mathrm{cm^2\,V^{-1}\,s^{-1}}. \quad (4)$$

In this equation, the donor density N_D is given in the unit of $\mathrm{cm^{-3}}$. Note that this curve is shown by a solid line in Fig. 3.

Another issue, which needs care, is incomplete ionization of dopants. The unipolar limit of a wide bandgap semiconductor has often been calculated by assuming complete ionization of dopants in previous reports. However, this is not correct because incomplete ionization of dopants at room temperature is rather common in wide bandgap semiconductors. The drift resistance is determined by the carrier density, whereas the electric field profile and thereby the breakdown voltage are determined by the doping density (not the carrier density). Therefore, the dopant ionization ratio, which is also dependent on the doping density, must be considered. In lightly-doped 4H-SiC, the ionization energies of nitrogen donors are 61 and 126 meV for a nitrogen atom substituting at the hexagonal and cubic sites, respectively.[2,29] In this study, the dependence of the ionization energies on the donor density[2] was also considered. The free electron density as a function of the nitrogen donor density in 4H-SiC was calculated at room temperature (300 K). As a result, nearly complete (>98%) ionization of donors is expected when the nitrogen density is below about $3 \times 10^{16}\,\mathrm{cm^{-3}}$. The ionization ratio of nitrogen donors decreases to about 80% or lower when the nitrogen density exceeds $2 \times 10^{17}\,\mathrm{cm^{-3}}$. This dependence was appropriately considered in the calculation of the on-resistance.

Taking account of the donor density dependences of electron mobility along ⟨0001⟩ and the free electron density, the specific on-resistances and breakdown voltage were calculated for both NPT and PT structures. Figure 4 depicts the trade-off relationship between the specific on-resistance of the drift layer and breakdown voltage in 4H-SiC{0001} unipolar devices. The results for the NPT and optimum PT structures are plotted by red dashed and solid lines, respectively. For comparison, the relationship calculated by assuming a fixed critical electric field strength of 2 or $3\,\mathrm{MV\,cm^{-1}}$ and a mobility of $1000\,\mathrm{cm^2\,V^{-1}\,s^{-1}}$, which have often been used in previous publications, is shown by blue dashed or solid lines, respectively. The "Si limit"[20] is also indicated by a black dashed line. As expected, the optimum PT structure yields a lower on-resistance than the NPT structure by 20%–25% at a given breakdown voltage. The on-resistance of the NPT structure (updated) is close to that assuming a fixed critical field strength of $3\,\mathrm{MV\,cm^{-1}}$ in the relatively low-voltage (<600 V) region and is close to that assuming a $2\,\mathrm{MV\,cm^{-1}}$ in the ultrahigh-voltage (>10 kV) region. This reflects the donor density dependence of the critical electric field strength shown in Fig. 1, where the critical field strength is approximately $3\,\mathrm{MV\,cm^{-1}}$ in the $10^{16}\,\mathrm{cm^{-3}}$ range and is about $2\,\mathrm{MV\,cm^{-1}}$ in the low $10^{15}\,\mathrm{cm^{-3}}$ range. The real "SiC limit", which should be defined by the on-resistance—breakdown voltage relationship for the optimum PT structure of 4H-SiC (red solid line in Fig. 5), is as low as 0.20, 2.5, 39 $\mathrm{m\Omega\,cm^2}$ for 1, 3, and 10 kV devices, respectively. This "SiC limit" can approximately be expressed by the following fitting equation:

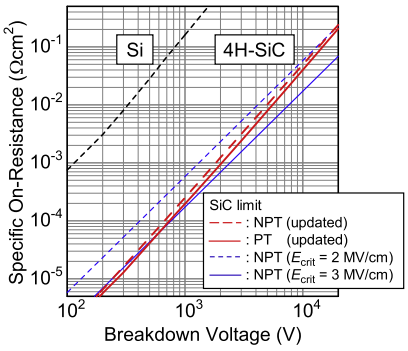

Fig. 4. (Color online) Trade-off relationship between the specific on-resistance of the drift layer and breakdown voltage in 4H-SiC{0001} unipolar devices. The results for the nonpunch-through (NPT) and optimum punch-through (PT) structures are plotted by red dashed and solid lines, respectively. For comparison, the relationship calculated by assuming a fixed critical electric field strength of 2 or $3\,\mathrm{MV\,cm^{-1}}$ and a mobility of $1000\,\mathrm{cm^2\,V^{-1}\,s^{-1}}$ is shown by blue dashed or solid line, respectively. The "Si limit"[20] is also indicated by a black dashed line.

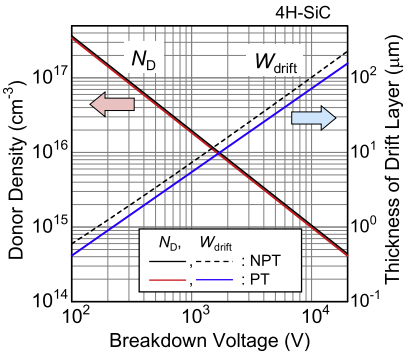

Fig. 5. (Color online) Donor density and thickness of the drift layer versus breakdown voltage for the NPT and optimum PT structures in 4H-SiC{0001} unipolar devices.

$$R_{on\_sp} = 2.95 \times 10^{-11}\,V_B^{2.28}\,\Omega\,\mathrm{cm^2}. \quad (5)$$

Here, the unit of V_B is V. The power exponent of the V_B term (2.28) is larger than 2 which is expressed in Eq. (1). This result again originates from the doping density dependence of the critical electric field strength. For achieving a higher breakdown voltage, the doping density of a drift layer must be reduced. This results in the decrease of critical electric field, as shown in Fig. 1, leading to the more rapidly-increasing on-resistance.

Figure 5 shows the donor density and thickness of the drift layer versus breakdown voltage for the NPT and optimum PT structures in 4H-SiC{0001} unipolar devices. As described in the introduction, the donor density and thickness for the NPT structure can be uniquely determined, provided that the accurate critical electric field strength as a function of doping density is given, and these are plotted by black solid and dashed lines, respectively. In the optimum PT structures which yield the best trade-off relationship shown by the red solid line in Fig. 4, the donor density and thickness are shown by red and blue solid lines, respectively. The donor density for the optimum PT structure is slightly lower than that for the NPT structure at a specified breakdown voltage, while the drift-layer thickness for the PT structure is significantly smaller than that for the NPT structure.

As indicated in Fig. 2, the electric field strength at the drift-layer end (E_{edge}) is expressed by xE_{max} $(0 < x \leqslant 1)$. The

present analysis revealed that the x value for the optimum PT structure in 4H-SiC{0001} unipolar devices is approximately 0.26 for 1–3 kV devices and is about 0.30 for 10–20 kV devices. Under a simple assumption that the critical field strength and mobility are independent of the doping density, it can be extracted mathematically that $x = 1/3(\approx 0.33)$ gives the optimum PT structure.[21)] However, the present study demonstrates that the optimum PT structure is obtained for $x = 0.26$–0.30. When various PT structures having the same breakdown voltage are compared, a lower x value means a higher doping density. Since the maximum electric field strength at breakdown increases by increasing the doping density as in the case of Fig. 1, the structure with a lower x value is more favorable than the PT structure with $x \approx 0.33$. This is the reason why the x values smaller than 0.33 yield the optimum PT structure in reality.

In summary, the trade-off relationship between the specific on-resistance and breakdown voltage in 4H-SiC{0001} unipolar devices was updated based on latest physical properties of the material. Optimum PT structures give about 20%–25% lower on-resistance than NPT structures at a specified breakdown voltage. The minimum specific on-resistances of 1 and 10 kV 4H-SiC devices are as low as 0.20 and 39 $m\Omega\,cm^2$, respectively, at room temperature. An analytical expression for the "SiC limit" was given. Although the on-resistance determined by the "SiC limit" is low, actual SiC power MOSFETs have exhibited much higher specific on-resistance, mainly due to poor channel mobility. Significant improvement of the channel mobility is crucial to reach the full potential of SiC.

Acknowledgments This work was supported by Council for Science, Technology and Innovation (CSTI), Cross-ministerial Strategic Innovation Promotion Program (SIP), "Next-generation power electronics/Consistent R&D of next-generation SiC power electronics" (funding agency: NEDO).

ORCID iDs Tsunenobu Kimoto https://orcid.org/0000-0002-6649-2090

1) B. J. Baliga, *Silicon Carbide Power Devices* (Singapore), (World Scientific Publishing, 2015).
2) T. Kimoto and J. A. Cooper, *Fundamentals of Silicon Carbide Technology* (Wiley, Singapore, 2014).

3) W. J. Choyke, H. Matsunami, and G. Pensl, (ed.), *Silicon Carbide, A Review of Fundamental Questions and Applications to Current Device Technology* Vols. I & II (Akademie Verlag, Berlin, 1997).
4) J. A., CooperJr. and A. Agarwal, Proc. IEEE **90**, 956 (2002).
5) T. Kimoto, Jpn. J. Appl. Phys. **54**, 040103 (2015).
6) H. Okumura, MRS Bulletin **40**, 439 (2015).
7) T. Kimoto and Y. Yonezawa, Mater. Sci. in Semiconductor Processing **78**, 43 (2018).
8) E. van Brunt, L. Cheng, M. J. O'Loughlin, J. Richmond, V. Pala, J. Palmour, C. W. Tipton, and C. Scozzie, Mater. Sci. Forum **847–850**, 847 (2015).
9) K. Nakayama, A. Tanaka, M. Nishimura, K. Asano, T. Miyazawa, M. Ito, and H. Tsuchida, IEEE Trans. Electron Devices **59**, 895 (2012).
10) N. Kaji, H. Niwa, J. Suda, and T. Kimoto, IEEE Trans. Electron Devices **62**, 374 (2015).
11) K. Hamada, S. Hino, N. Miura, H. Watanabe, S. Nakata, E. Suekawa, Y. Ebiike, M. Imaizumi, I. Umezaki, and S. Yamakawa, Jpn. J. Appl. Phys. **54**, 04DP07 (2015).
12) T. Nakamura, Y. Nakano, M. Aketa, R. Nakamura, S. Mitani, H. Sakairi, and Y. Yokotsuji, Tech. Digest of 2011 Int. Electron Devices Meeting (San Francisco, USA, 2011), 26.5.1.
13) K. Uchida et al., Proc. 27th Int. Symp. on Power Semiconductor Devices & IC's (Hong Kong, China, 2015), p. 85.
14) J. W. Palmour, Tech. Digest of 2014 Int. Electron Devices Meeting (San Francisco, USA, 2014), 1.1.
15) S. Harada, M. Kato, K. Suzuki, M. Okamoto, T. Yatsuo, K. Fukuda, and K. Arai, Tech. Digest of 2006 Int. Electron Devices Meeting (San Francisco, USA, 2006), p 903.
16) A. Ichimura, Y. Ebihara, S. Mitani, M. Noborio, Y. Takeuchi, S. Mizuno, T. Yamamoto, and K. Tsuruta, Mater. Sci. Forum **924**, 707 (2018).
17) M. Bhatnagar and B. J. Baliga, IEEE Trans. Electron Devices **40**, 645 (1993).
18) T. Kachi, Jpn. J. Appl. Phys. **53**, 100210 (2014).
19) S. Fujita, Jpn. J. Appl. Phys. **54**, 030101 (2015).
20) B. J. Baliga, *Fundamentals of Power Semiconductor Devices* (Springer, Berlin, 2008).
21) D. A. Grant and J. Gower, *Power MOSFETs: Theory and Applications* (Wiley, New York, 1989).
22) S. Nakamura, H. Kumagai, T. Kimoto, and H. Matsunami, Appl. Phys. Lett. **80**, 3355 (2002).
23) T. Hatakeyama, T. Watanabe, T. Shinohe, K. Kojima, K. Arai, and N. Sano, Appl. Phys. Lett. **85**, 1380 (2014).
24) T. Fujihira, Jpn. J. Appl. Phys. **36**, 6254 (1997).
25) H. Niwa, J. Suda, and T. Kimoto, IEEE Trans. Electron Devices **62**, 3326 (2015).
26) T. Kimoto, H. Niwa, T. Okuda, E. Saito, Y. Zhao, S. Asada, and J. Suda, J. Phys. D: Appl. Phys. **51**, 363001 (2018).
27) W. J. Schaffer, G. H. Negley, K. G. Irvine, and J. W. Palmour, Mater. Res. Soc. Symp. Proc. **339**, 595 (1994).
28) S. Kagamihara, H. Matsuura, T. Hatakeyama, T. Watanabe, M. Kushibe, T. Shinohe, and K. Arai, J. Appl. Phys. **96**, 5601 (2004).
29) I. G. Ivanov, A. Henry, and E. Janzen, Phys. Rev. B **71**, 241201 (2005).